

De Novo Mutations in *GNAO1*, Encoding a $G\alpha_o$ Subunit of Heterotrimeric G Proteins, Cause Epileptic Encephalopathy

Kazuyuki Nakamura,^{1,2,9} Hirofumi Kodera,^{1,9} Tenpei Akita,^{3,9} Masaaki Shiina,⁴ Mitsuhiro Kato,² Hideki Hoshino,⁵ Hiroshi Terashima,⁵ Hitoshi Osaka,⁶ Shinichi Nakamura,⁷ Jun Tohyama,⁸ Tatsuro Kumada,³ Tomonori Furukawa,³ Satomi Iwata,³ Takashi Shiihara,^{2,10} Masaya Kubota,⁵ Satoko Miyatake,¹ Eriko Koshimizu,¹ Kiyomi Nishiyama,¹ Mitsuko Nakashima,¹ Yoshinori Tsurusaki,¹ Noriko Miyake,¹ Kiyoshi Hayasaka,² Kazuhiro Ogata,⁴ Atsuo Fukuda,³ Naomichi Matsumoto,^{1,*} and Hiroto Saito^{1,*}

Heterotrimeric G proteins, composed of α , β , and γ subunits, can transduce a variety of signals from seven-transmembrane-type receptors to intracellular effectors. By whole-exome sequencing and subsequent mutation screening, we identified de novo heterozygous mutations in *GNAO1*, which encodes a $G\alpha_o$ subunit of heterotrimeric G proteins, in four individuals with epileptic encephalopathy. Two of the affected individuals also showed involuntary movements. Somatic mosaicism (approximately 35% to 50% of cells, distributed across multiple cell types, harbored the mutation) was shown in one individual. By mapping the mutation onto three-dimensional models of the $G\alpha$ subunit in three different complexed states, we found that the three mutants (c.521A>G [p.Asp174Gly], c.836T>A [p.Ile279Asn], and c.572_592del [p.Thr191_Phe197del]) are predicted to destabilize the $G\alpha$ subunit fold. A fourth mutant (c.607G>A), in which the Gly203 residue located within the highly conserved switch II region is substituted to Arg, is predicted to impair GTP binding and/or activation of downstream effectors, although the p.Gly203Arg substitution might not interfere with $G\alpha$ binding to G-protein-coupled receptors. Transient-expression experiments suggested that localization to the plasma membrane was variably impaired in the three putatively destabilized mutants. Electrophysiological analysis showed that $G\alpha_o$ -mediated inhibition of calcium currents by norepinephrine tended to be lower in three of the four $G\alpha_o$ mutants. These data suggest that aberrant $G\alpha_o$ signaling can cause multiple neurodevelopmental phenotypes, including epileptic encephalopathy and involuntary movements.

Introduction

Epileptic encephalopathy is a group of neurological disorders characterized by severe and progressive cognitive and behavioral impairments, which are most likely caused or made worse by epileptic activity.¹ Ohtahara syndrome (OS [MIM 308350 and 612164]) is the most severe and the earliest form of epileptic encephalopathy and is characterized by tonic spasms mainly in the neonatal period, seizure intractability, and a suppression-burst pattern on electroencephalography (EEG).² De novo mutations in three genes, *ARX* (MIM 300382), *STXBPI* (MIM 602926), and *KCNQ2* (MIM 602235), have been reported in individuals with OS.^{3–6}

Heterotrimeric guanine-binding proteins (G proteins) are composed of α , β , and γ subunits. In its basal state, $G\alpha$ is bound with guanosine diphosphate (GDP) and forms the $G\alpha\beta\gamma$ complex. When a seven-transmembrane-type receptor binds its agonist, it activates G proteins by cata-

lyzing the exchange of GDP for guanosine triphosphate (GTP) on the $G\alpha$ subunit. Subsequently, GTP-bound $G\alpha$ dissociates from $G\beta\gamma$, and each of the two complexes activates distinct downstream effectors.⁷ In mammals, $G\alpha$ subunits are divided into four classes: $G\alpha_{i/o}$, $G\alpha_{q/11}$, $G\alpha_s$, and $G\alpha_{12/13}$.⁷ $G\alpha_o$, encoded by *GNAO1* (MIM 139311), is extremely abundant in brain tissue, where it can constitute up to approximately 0.5% of membrane protein,⁸ suggesting important roles in brain function. In fact, mice lacking $G\alpha_o$ show multiple neurological abnormalities, including generalized tremor, occasional seizures, severe motor-control impairment, hyperalgesia, and behavioral abnormalities with early postnatal lethality.^{9,10}

In this study, de novo *GNAO1* mutations were identified in four epileptic-encephalopathy-affected individuals, three of whom were diagnosed with OS. In addition, two of the four individuals showed involuntary movements, suggesting that aberration of $G\alpha_o$ can cause multiple neurodevelopmental phenotypes.

¹Department of Human Genetics, Yokohama City University Graduate School of Medicine, 3-9 Fukuura, Kanazawa-ku, Yokohama 236-0004, Japan; ²Department of Pediatrics, Yamagata University Faculty of Medicine, 2-2-2 Iida-nishi, Yamagata 990-9585, Japan; ³Department of Neurophysiology, Hamamatsu University School of Medicine, 1-20-1 Handayama, Higashi-ku, Hamamatsu 431-3192, Japan; ⁴Department of Biochemistry, Yokohama City University Graduate School of Medicine, 3-9 Fukuura, Kanazawa-ku, Yokohama 236-0004, Japan; ⁵Division of Neurology, National Center for Child Health and Development, 2-10-1 Okura, Setagaya-ku, Tokyo 157-8535, Japan; ⁶Division of Neurology, Clinical Research Institute, Kanagawa Children's Medical Center, 2-138-4 Mutsukawa, Minami-ku, Yokohama 232-8555, Japan; ⁷Department of Pediatrics, Nagano Red Cross Hospital, 5-22-1 Wakasato, Nagano 380-8582, Japan; ⁸Department of Pediatrics, Epilepsy Center, Nishi-Niigata Chuo National Hospital, Niigata 950-2085, Japan

⁹These authors contributed equally to this work

¹⁰Present address: Department of Neurology, Gunma Children's Medical Center, 779 Shimohakoda Hakkitsu-machi, Shibukawa, Gunma 377-8577, Japan

*Correspondence: naomat@yokohama-cu.ac.jp (N.M.), hsaito@yokohama-cu.ac.jp (H.S.)

<http://dx.doi.org/10.1016/j.ajhg.2013.07.014>. ©2013 by The American Society of Human Genetics. All rights reserved.

Subjects and Methods

Subjects

Twelve individuals with OS were previously analyzed by whole-exome sequencing (WES).^{3,11} In addition, we analyzed parental samples from 5 of the 12 individuals by WES. Screening for *GNAO1* mutations was performed in 367 individuals with epileptic encephalopathy (including 62 OS cases) by high-resolution-melting (HRM) analysis (339 cases) and/or WES (100 cases). The diagnosis was made on the basis of clinical features and characteristic patterns on EEG. Experimental protocols were approved by the institutional review board of Yokohama City University School of Medicine and Yamagata University Faculty of Medicine. Informed consent was obtained from the families of all individuals.

DNA Samples

Genomic DNA was obtained from peripheral-blood leukocytes by standard methods. For detection of a mosaic mutation in individual 2, genomic DNA from saliva and nails was isolated with an Oragene DNA kit (DNA Genotek) and an ISOHAIR kit (Nippon Gene), respectively.

WES

Genomic DNA was captured with the SureSelect Human All Exon v.4 Kit (Agilent Technologies) and sequenced with four samples per lane on an Illumina HiSeq 2000 (Illumina) with 101 bp paired-end reads. Image analysis and base calling were performed by Sequencing Control Software with Real-Time Analysis and CASAVA software v.1.8 (Illumina). Exome data processing, variant calling, and variant annotation were performed as previously described.^{12–14} Reads were aligned to GRCh37 with Novoalign (Novocraft Technologies). Duplicate reads were removed with Picard, and local realignments around indels and base-quality-score recalibration were performed with the Genome Analysis Toolkit (GATK).¹³ Single-nucleotide variants and small indels were identified with the GATK UnifiedGenotyper and were filtered according to the Broad Institute's best-practice guidelines v.3. Not flagged as clinically associated, variants registered in dbSNP135 were filtered. Filter-passed variants were annotated with ANNOVAR.¹⁴ Pathogenic mutations detected by WES were confirmed by Sanger sequencing.

Mutation Screening

Genomic DNA was amplified with an illustra GenomiPhi V2 DNA Amplification Kit (GE Healthcare). Exons 1–8 covering the *GNAO1* coding region of two transcript variants (transcript variant 1, RefSeq accession number NM_020988.2, encoding $G\alpha_{o1}$; transcript variant 2, RefSeq accession number NM_138736.2, encoding $G\alpha_{o2}$) were screened by HRM analysis. The last two exons differ between the transcript variants. HRM analysis was performed with a Light Cycler 480 (Roche Diagnostics). Samples showing an aberrant melting curve in the HRM analysis were sequenced. PCR primers and conditions are shown in Table S1, available online. All mutations not present in publically available databases were verified with original genomic DNA and were searched for in the variant database of our 408 in-house control exomes.

Deep Sequencing of a Mosaic Mutation

PCR products (length 178 bp) spanning the c.521A>G mutation were amplified with the use of blood, saliva, and nail DNA samples

from individual 2 and blood DNA samples from her parents as a template. Adaptor ligation, nick repair, and amplification were performed with the Ion Xpress Plus Fragment Library Kit (Life Technologies) according to the manufacturer's protocol (part no. 4471989 Rev. B). Indexing was carried out with the Xpress Barcode Adapters 1–16 Kit (Life Technologies). Emulsion PCR and enrichment steps were carried out with the Ion OneTouch 200 Template Kit v.2 (Life Technologies) according to the manufacturer's protocol (part no. 4478371 Rev. A). Sequencing of the amplicon libraries was carried out on the Ion Torrent Personal Genome Machine (PGM) with the Ion 314 sequencing chip and the Ion PGM 200 Sequencing Kit (Life Technologies) according to the recommended protocol (part no. 4474246 Rev. B). Torrent Suite 2.2 was used for all analyses. The percentage of mosaicism was examined with the Integrative Genomics Viewer.^{15,16}

Expression Vectors

A full-length human *GNAO1* cDNA clone (transcript variant 1, encoding $G\alpha_{o1}$) was purchased from Kazusa DNA Research Institute. Human *GNAO1* cDNA was inserted into a pEF6/V5-His-C vector for the introduction of a C-terminal V5 epitope (Life Technologies). Site-directed mutagenesis using a KOD-Plus-Mutagenesis kit (Toyobo) was performed for generating *GNAO1* mutants, including c.521A>G (p.Asp174Gly), c.572_592del (p.The191_Phe197del), c.836T>A (p.Ile279Asn), and c.607G>A (p.Gly203Arg). A c.607_609delinsACA (p.Gly203Thr) mutant, in which GTP binding was reversible in contrast to the WT,¹⁷ was also generated to serve as the known loss-of-function mutant.¹⁸ All variant cDNAs were confirmed by Sanger sequencing.

Immunofluorescence Microscopy

Mouse neuroblastoma 2A (N2A) cells were grown as previously described.⁴ N2A cells on glass coverslips were transfected with 200 ng of plasmid DNA with the use of X-tremeGENE 9 DNA Transfection Reagent (Roche Diagnostics). After 24 hr, cells were fixed in PBS containing 4% paraformaldehyde for 15 min and permeabilized in PBS containing 0.1% Triton X-100 for 5 min. Cells were then blocked with 10% normal goat serum for 30 min. V5-tagged $G\alpha_{o1}$ was detected with a mouse V5 antibody (1:200 dilution; Life Technologies) and Alexa-488-conjugated goat anti-mouse IgG (1:1000 dilution; Life Technologies). Coverslips were mounted with Vectashield (Vector Laboratories) that contained DAPI and were visualized with an inverted FV1000-D confocal microscope (Olympus).

Structural Modeling and Free-Energy Calculations

We used FoldX software (version 3.0β5) to construct mutated molecular structures and calculate the free-energy changes caused by the mutations.¹⁹ We used crystal structures of the GDP-bound inactive $G\alpha_i\beta\gamma$ heterotrimer (Protein Data Bank [PDB] 1GG2),²⁰ the nucleotide-free $G\alpha_s\beta\gamma$ in complex with agonist-occupied monomeric β_2 adrenergic receptor (β_2 AR) (PDB 3SN6),²¹ and the transition-state analog of GTP (GDP⁺AlF₄⁻)-bound $G\alpha_q$ in complex with its effector phospholipase C- β (PLC β) (PDB 3OHM)²² as three-dimensional structure models of the $G\alpha_o$ subunit in different complexed states. Each of the mutations, corresponding to p.Asp174Gly, p.Ile279Asn, or p.Gly203Arg in the human $G\alpha_o$ subunit, was introduced into the $G\alpha$ subunit of each complex, and the free-energy change upon the mutation was calculated with FoldX software. Note that ligands included in the complexes were ignored in the calculation because the FoldX energy function

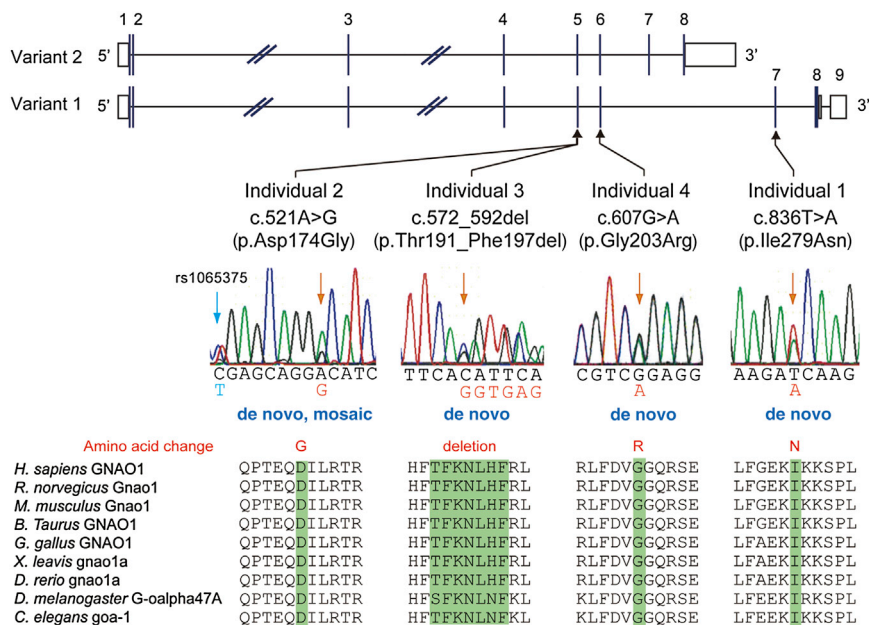


Figure 1. De Novo GNAO1 Mutations in Individuals with Epileptic Encephalopathy Schematic representation of GNAO1, including two transcript variants: transcript variant 1 (RefSeq NM_020988.2) with nine exons and transcript variant 2 (RefSeq NM_138736.2) with eight exons. The UTRs and coding regions are shown in white and black rectangles, respectively. Three mutations occurred in common exons of two transcript variants, and one mutation occurred uniquely in transcript variant 1. Note that the electropherogram of individual 2 suggested mosaicism of the c.521A>G mutation, and a heterozygous C>T change (rs1065375) was clearly demonstrated. All mutations caused substitution or deletion of evolutionarily conserved amino acids. Homologous sequences were aligned with the use of the CLUSTALW web site.

does not consider the contribution of ligands. The calculation was repeated three times, and the resultant data were presented as an average value with a SD.

Electrophysiology

For electrophysiological recording of calcium currents, we used NG108-15 cells transfected with individual GNAO1 mutants. Expression vectors were introduced by electroporation with the Lonza Nucleofector device and the Cell Line Nucleofector Kit V (Lonza) according to the manufacturer's protocol (program X-023). Two micrograms of plasmid DNA was used per transfection. The transfected cells were plated on poly-L-lysine-coated plastic coverslips (Cell Desk LF, MS-0113L; Sumitomo Bakelite) at a density of about 5×10^4 cells/cm² and cultured in Dulbecco's modified Eagle's medium (DMEM) supplemented with 10% fetal bovine serum (FBS). One day after transfection, the cells were differentiated with DMEM supplemented with 10 μ M prostaglandin E1, 50 μ M IBMX, and 1% FBS for 3–7 days before recording. During the culture period, half of the medium was changed every other day.

The recording was made by the perforated whole-cell patch-clamp technique with amphotericin B. Cells on coverslips were perfused under an Olympus BX51W upright microscope (Olympus) with a bath solution containing 140 mM NaCl, 5 mM CaCl₂, 4 mM KCl, 1 mM MgCl₂, 10 mM HEPES, 10 mM TEACl, 8 mM glucose, and 0.0002 mM tetrodotoxin (pH 7.3 adjusted with NaOH). The patch pipette solution contained 100 mM CsCl, 10 mM EGTA, and 40 mM HEPES (pH 7.3 adjusted with CsOH). Amphotericin B was added to the pipette solution at 2 μ l/ml just before the experiments. The pipettes were fabricated from borosilicate glass capillaries and had a resistance of 4–8 M Ω when backfilled with the amphotericin-B-containing pipette solution. The recording was started when the series resistance was reduced to <150 M Ω after gigaseal formation and clear cellular capacitive surges had appeared. Voltage-gated calcium currents were elicited by the application of 50 ms depolarizing pulses to +10 mV from the holding potential of –65 mV, recorded with a Multiclamp 700B (Molecular Devices) controlled via

pCLAMP10 software (Molecular Devices), filtered at 2 kHz, and sampled at 10 kHz with 50% compensation for series resistance. G α_o -mediated current inhibition was elicited by the application of 10 μ M norepinephrine via the bath solution. After 3–5 min, inhibition was assessed by measurement of the changes in current density just before the end of the depolarizing pulses. Recordings were made at room temperature.

Statistical multiple comparisons were made with ANOVA followed by Dunnett's post hoc test, and the threshold p value for judging statistical significance was 0.05. The current inhibition induced by norepinephrine in individual mutant-expressing cells was assessed with a paired t test. The results are given as the mean \pm SEM.

Results

GNAO1 Is Mutated in Individuals with Epileptic Encephalopathy

We previously performed WES of 12 individuals with OS.^{3,11} In this study, we analyzed parental samples from 5 of the 12 individuals by WES (mean RefSeq read depth of 109) to systematically screen de novo or recessive mutations. We found no recessive mutations in SLC25A22 (MIM 609302), PNPO (MIM 610090), PNKP (MIM 613402), PLCB1 (MIM 613722), or ST3GAL3 (MIM 615006), whose mutations were previously found in epileptic encephalopathy,^{23–27} but we did find one or two de novo mutations in each of the five trio exomes. Among them, a de novo missense mutation (c.836T>A [p.Ile279Asn]) in GNAO1 at 16q12.2 was identified in individual 1. In the exome data of the other seven original individuals, we also found in individual 2 a second missense mutation (c.521A>G [p.Asp174Gly]), which was confirmed as a de novo event by Sanger sequencing (Figure 1). Moreover, GNAO1 mutation screening in 367 individuals with epileptic encephalopathy by HRM analysis (339 individuals) and/or WES (100 individuals,

Table 1. Clinical Features of Individuals with a *GNAO1* Mutation

	Individual 1	Individual 2	Individual 3	Individual 4
Gender	female	female	female	female
Age	13 years	4 years, 1 month	died at 11 months	8 years
Mutation	c.836T>A (p.Ile279Asn)	c.521A>G (p.Asp174Gly)	c.572_592 del (p.Thr191_Phe197 del)	c.607G>A (p.Gly203Arg)
Inheritance	de novo	de novo, somatic mosaic	de novo	de novo
Diagnosis	Ohtahara syndrome	Ohtahara syndrome	Ohtahara syndrome	epileptic encephalopathy
Initial symptom	tonic seizure at 4 days	series of tonic seizures at 29 days (tonic upgaze, head nodding, extension of all extremities)	series of tonic seizures at 2 weeks (resemble spasms)	opisthotonic posture, developmental delay at 7 months
Initial EEG	suppression-burst pattern at 4 days	suppression-burst pattern at 29 days	suppression-burst pattern at 2 weeks	diffuse irregular spike-and-slow-wave complex at 5 years
Course of seizures	tonic seizure at 5 years	series of tonic seizures at 9 months	tonic seizure at 10 months	focal seizure (tonic upgaze), tonic seizure at 5 years
Course of EEG	multifocal sharp waves at 1 year, 4 months; suppression-burst pattern at 5 years, 6 months	hypsarrhythmia at 3 months; diffuse spike-and-slow-wave complex at 1 year, 7 months; sharp waves at frontal lobe at 3 years, 9 months	hypsarrhythmia at 4 months	not done
Involuntary movement	-	-	dystonia	severe chorea, athetosis
Seizure control	intractable (2–3 times per day)	intractable (0–2 times per day)	intractable	intractable (several times per day)
Development				
Head control	-	+	-	-
Sitting	-	-	-	-
Meaningful words	-	-	-	-
MRI	normal at 1 month; cerebral atrophy at 5 years, 6 months	delayed myelination and thin corpus callosum at 10 months	normal at 3 months	delayed myelination at 1 year, 3 months; reduced cerebral white matter, thin corpus callosum at 4 years, 8 months

mean read depth of 129) revealed two de novo mutations: c.572_592 del (p.Thr191_Phe197del) in individual 3 and c.607G>A (p.Gly203Arg) in individual 4 (Figure 1). One mutation (c.836T>A) specifically affects *GNAO1* transcript variant 1, whereas the other three mutations affect both transcript variants 1 and 2. Web-based prediction tools suggested that these four mutations would be pathogenic (Table S2). None of the four mutations was found in the 6,500 exomes of the National Heart, Lung, and Blood Institute (NHLBI) Exome Sequencing Project Exome Variant Server or among our 408 in-house control exomes. Interestingly, exome data and Sanger sequencing indicated that the c.521A>G mutation in individual 2 was somatic mosaic (Figure 1 and Table S3). We confirmed de novo somatic mosaicism of the c.521A>G mutation by deep sequencing of PCR products amplified with blood, nail, and saliva DNA from individual 2 and blood DNA from her parents, showing that approximately 35%–50% of cells harbored the mutation (Table S3).

Phenotypes Associated with *GNAO1* Mutations

Neurological features of four female individuals with *GNAO1* mutations are shown in Table 1. Three individuals (individuals 1–3) developed tonic seizures with suppression-burst pattern on EEG at the onset (range 4–29 days), leading to a diagnosis of OS. Individuals 2 and 3 transitioned to West syndrome, a common infantile epileptic syndrome, as revealed by hypsarrhythmia on EEG at 3–4 months of age (Figures 2A–2C). Individual 4 showed developmental delay and opisthotonic posture at 7 months of age, and complex partial seizures with epileptic discharge on EEG was observed at 5 years (Figure 2D). Of note, two individuals showed involuntary movements: individual 3 showed dystonia, and individual 4 displayed chorea and athetosis (Table 1 and Movie S1). Brain MRI showed delayed myelination in individuals 2 and 4, cerebral atrophy or reduced cerebral white matter in individuals 1 and 4, and thin corpus callosum in individuals 2 and 4 (Figures 2E–2I). Although seizures and EEG

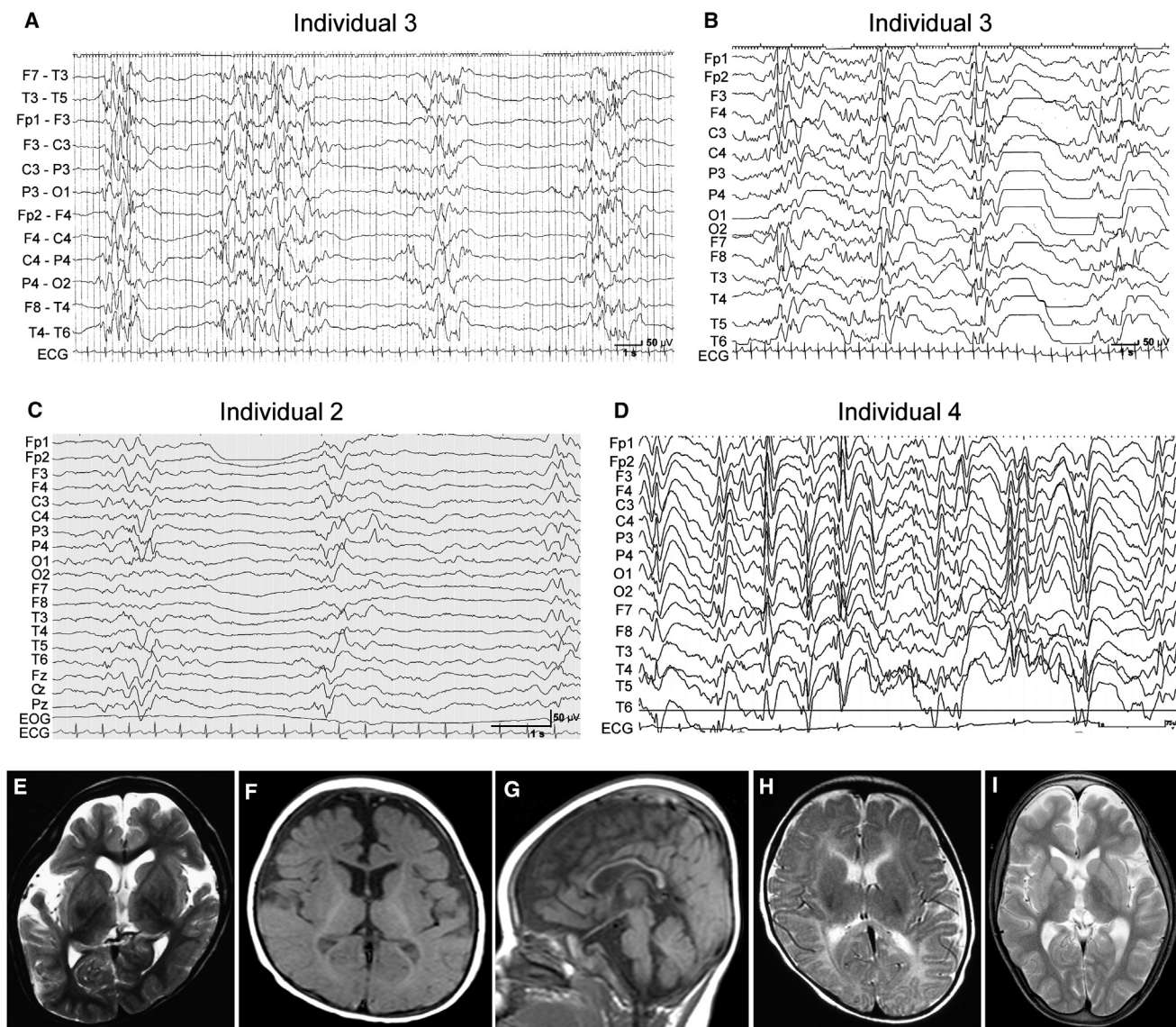


Figure 2. EEG and Brain MRI Features of Individuals with *GNAO1* Mutations

(A and B) Interictal EEG of individual 3. A suppression-burst pattern was observed at 2 months of age (A), and transition to hypsarrhythmia was observed at 4 months (B).

(C) Interictal EEG of individual 2 shows a suppression-burst pattern at 2 months.

(D) Interictal EEG of individual 4 shows a diffuse spike- or sharp-and-slow-wave complex at 5 years.

(E–I) T2-weighted axial images through the basal ganglia (E, H, and I) and T1-weighted axial (F) and sagittal (G) images. Individual 1 showed cerebral atrophy at 5 years and 6 months (E). Individual 2 showed delayed myelination and thin corpus callosum at 10 months (F and G). Individual 3 showed normal appearance at 3 months (H). Individual 4 showed reduced white matter at 7 years (I).

findings in two individuals with OS (individuals 2 and 3) were temporarily improved by adrenocorticotrophic hormone therapy and valproic acid, all four individuals had intractable epileptic seizures in spite of combinatory therapy of antiepileptic drugs. All individuals had severe intellectual disability and motor developmental delay, and individual 3 died at 11 months because of respiratory-tract obstruction. These data suggest that *GNAO1* mutations can cause multiple neurodevelopmental phenotypes, including epileptic encephalopathy and involuntary movements.

Expression of Mutant $G\alpha_{o1}$ in N2A Cells

To examine the mutational effect of four *GNAO1* mutations, we performed transient expression experiments in N2A cells (Figure 3). C-terminally V5-epitope-tagged wild-type (WT) $G\alpha_{o1}$, encoded by transcript variant 1, was clearly localized in the cell periphery, as previously reported.²⁸ The p.Gly203Thr (with known loss of function)¹⁷ and p.Gly203Arg (in individual 4) altered proteins were also localized in the cell periphery. In contrast, the p.Thr191_Phe197del altered protein (in individual 3) accumulated in the cytosolic compartment. The p.Asp174Gly

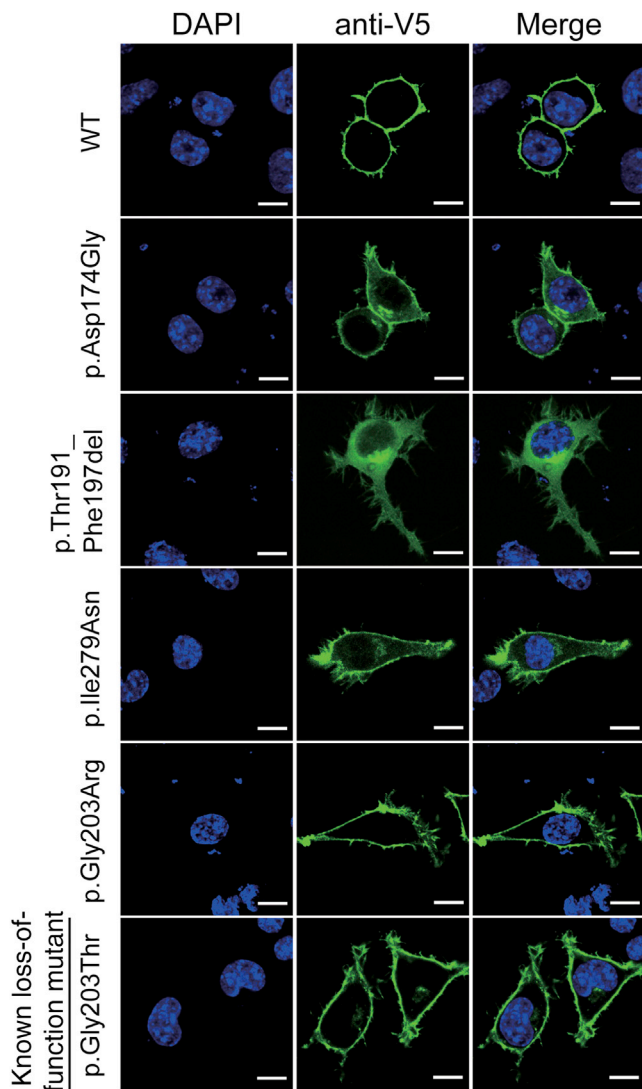


Figure 3. Localization of V5-Tagged $G\alpha_{o1}$ Proteins in N2A Cells
 Localization of WT and five altered $G\alpha_{o1}$ proteins in N2A cells. The WT and p.Gly203Arg and p.Gly203Thr altered proteins were localized to the cell periphery. In contrast, the p.Thr191_Phe197del protein was localized to the cytosolic compartment. The other p.Asp174Gly and p.Ile279Asn proteins were localized to the cell periphery but were also observed in the cytosol. The scale bars represent 10 μm .

(individual 2) and p.Ile279Asn (individual 1) altered proteins were localized to the cell periphery and had weak signal in the cytosol, where more intense signal was observed in the p.Asp174Gly protein. Similar patterns of localization were observed for C-terminally AcGFP1-tagged $G\alpha_{o1}$ (Figure S1). These localization patterns suggest that the function of the p.Thr191_Phe197del altered protein might be most severely affected.

Structural Impacts of the Mutations on the $G\alpha$ -Containing Complexes

To evaluate the impact of the *GNAO1* mutations on specific functions at the atomic level, we mapped the substituted positions onto structures of the $G\alpha$ subunit in

complexed states representing the GDP-bound inactive state, the nucleotide-free $G\alpha_s\beta\gamma$ in complex with the receptor, and the GTP-bound active state. In the case of point mutations, we further estimated free-energy changes of the mutations by using FoldX software (version 3.0 β 5).¹⁹

The region corresponding to amino acid residues 191–197 of human $G\alpha_{o1}$ is located in β strands and their connecting loop region and is involved in interactions with the G-protein-coupled receptor (GPCR) in the $G\alpha\beta\gamma$ - β 2AR complex (Figure 4A and Figure S2A). Thus, the deletion would affect secondary structure of the molecule and would not only impair the interaction with GPCR but also severely destabilize the $G\alpha$ -subunit fold. The substituted residues corresponding to Asp174 and Ile279 of the human $G\alpha_{o1}$ subunit are both buried inside the protein (Figure 4A) and are involved in hydrogen-bonding and hydrophobic interactions, respectively (Figure S2B). Therefore, the p.Asp174Gly and p.Ile279Asn substitutions would destabilize the $G\alpha$ -subunit fold, as supported by FoldX calculations showing a more than 2 kcal/mol increase in free-energy changes for these substitutions (Figure 4B). It can be speculated that these altered proteins tend to be misfolded or denatured in N2A cells and thus have altered cellular localization (Figure 3).

The substituted residue corresponding to Gly203 of human $G\alpha_{o1}$ is located within the highly conserved switch II region, responsible for activation of downstream effectors upon GTP binding (Figure 4A). Conformations of the switch regions differ depending on the complex state of the G protein. In the $G\alpha\beta\gamma$ heterotrimer and the GDP⁺AlF₄⁻-bound $G\alpha$ -effector (PLC β) complex, the glycine residues are closely surrounded by the switch I region and GTP (Figure 4A and Figure S2C). Thus, the p.Gly203Arg substitution would cause steric hindrance between the arginine side chain and the switch I region and/or GTP, destabilizing the complex, as supported by the FoldX calculations showing a remarkable increase in free-energy change upon the p.Gly203Arg substitution. By contrast, in the $G\alpha\beta\gamma$ -receptor (β 2AR) complex, no substantial steric hindrance was predicted from the structural modeling and FoldX calculations (Figure 4B and Figure S2C). These findings suggest that the p.Gly203Arg-substituted $G\alpha$ subunit would impair GTP binding and/or activation of the downstream effectors, although it might still bind to GPCR. This prediction was supported by previous reports, in which GTP binding was weakened in the p.Gly203Thr altered $G\alpha$.¹⁷ This also appears to be consistent with the apparently normal cellular localization of the p.Gly203Arg altered protein in N2A cells (Figure 3).

Electrophysiological Evaluation of $G\alpha_{o1}$ Mutants

It has been reported that N-type calcium channels are inhibited, at least in part, via $G\alpha_o$ -mediated signaling.⁷ Using NG108-15 cells, in which norepinephrine-induced calcium-current inhibition is mediated by $G\alpha_o$ (Figure 5A),²⁹ we analyzed functional properties of altered $G\alpha_{o1}$. Compared with cells expressing WT $G\alpha_{o1}$ (the

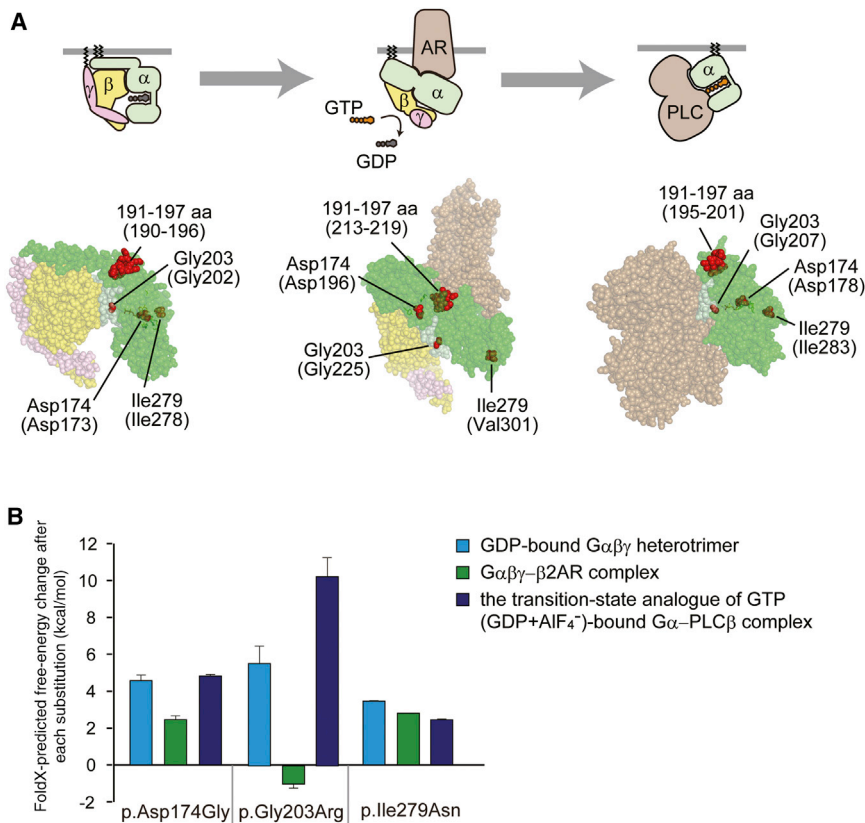


Figure 4. Structural Consideration of the $G\alpha$ Amino Acid Substitutions in Some Complexed States

(A) Map of the amino acid substitution sites on the crystal structures of $G\alpha$ -containing complexes: the GDP-bound inactive $G\alpha\beta\gamma$ heterotrimer (left), the nucleotide-free $G\alpha\beta\gamma$ in complex with an agonist-occupied monomeric β 2AR (center), and the $GDP+AlF_4$ -bound $G\alpha$ in complex with its effector PLC β (right). Molecular structures are shown as space-filling representations (from PyMOL). $G\alpha$, $G\beta$, and $G\gamma$ subunits are colored green, yellow, and pink, respectively, and the switch I and switch II regions in the $G\alpha$ subunit are in light green. The β 2AR (center) and PLC β (right) molecules are colored brown. The substituted sites are shown in red, and the indicated amino acid numbers correspond to human $G\alpha_{o1}$ and, in parentheses, rat $G\alpha_{i1}$ (UniProtKB/Swiss-Prot P10824) (left), bovine $G\alpha_s$ (UniProtKB/Swiss-Prot P04896) (center), and mouse $G\alpha_q$ (UniProtKB/Swiss-Prot P21279) (right). The illustrations above each model show the orientation of each subunit and the bound molecules.

(B) The free-energy change after each of the amino acid substitutions was estimated from calculations using FoldX software. Each error bar represents an average value with a SD.

leftmost column in Figure 5B), NG108-15 cells expressing the p.Thr191_Phe197del substitution revealed a significant increase in calcium-current density before application of norepinephrine ($p < 0.05$ by Dunnett's post hoc test; the second column from the right in Figure 5B), suggesting that localization of the altered $G\alpha_{o1}$ might affect calcium-channel activity. In cells expressing the p.Asp174Gly substitution, a mild increase in the current density was also suggested, although the difference was not significant (the third column from the left in Figure 5B). The other two substitutions had no effects on the current (the second column from the left and the rightmost column in Figure 5B). Treatment with 10 μ M norepinephrine reduced the calcium-current density by $19.0\% \pm 5.0\%$ in cells expressing WT $G\alpha_{o1}$ ($p < 0.01$ by paired t test; left panel in Figure 5A and the leftmost bar in Figure 5C). A similar reduction was observed in cells expressing the p.Ile279Asn alteration ($18.5\% \pm 3.5\%$, $p < 0.01$ by paired t test; the rightmost bar in Figure 5C). In cells expressing the p.Thr191_Phe197del alteration, by contrast, the reduction was obscured ($12.1\% \pm 5.0\%$, not significant by paired t test; right panel in Figure 5A and the second bar from the right in Figure 5C). In cells expressing the other two substitutions (p.Gly203Thr and p.Asp174Gly), weaker current inhibition by norepinephrine was suggested ($9.9\% \pm 3.8\%$ and $11.1\% \pm 3.5\%$, respectively; both were $p < 0.05$ by paired t test; the second and third bars from the left in Figure 5C), although compared with that in WT-expressing cells, the degrees

of inhibition in Gly203Thr- and p.Asp174Gly-expressing cells did not reach statistical significance (not significant by ANOVA). These data suggest that $GNAO1$ mutations could hamper $G\alpha_o$ -mediated signaling.

Discussion

We successfully identified four de novo heterozygous missense $GNAO1$ mutations in four individuals. All four individuals showed severe intellectual disability and motor developmental delay, demonstrating that aberration of $G\alpha_o$ affects intellectual and motor development. In addition, all four individuals showed epileptic encephalopathy, and two of them showed involuntary movements. Because $G\alpha_o$ -deficient mice show occasional seizures and generalized tremor,^{9,10} it is likely that epilepsy and involuntary movement are two of the characteristic features caused by $GNAO1$ mutations. Although $G\alpha_o$ -deficient mice also show hyperactivity and hyperalgesia,¹⁰ it is difficult to evaluate whether our individuals had these symptoms because of severe motor and cognitive impairment.

All four of these mutations, and especially two mutations leading to the p.Thr191_Phe197del and p.Gly203Arg substitutions, are predicted to affect $G\alpha_o$ function by structural evaluation. In fact, transient expression in N2A cells showed that localization of the p.Thr191_Phe197del altered protein was dramatically changed to the cytosolic compartment. Interestingly, two alterations (p.Ile279Asn

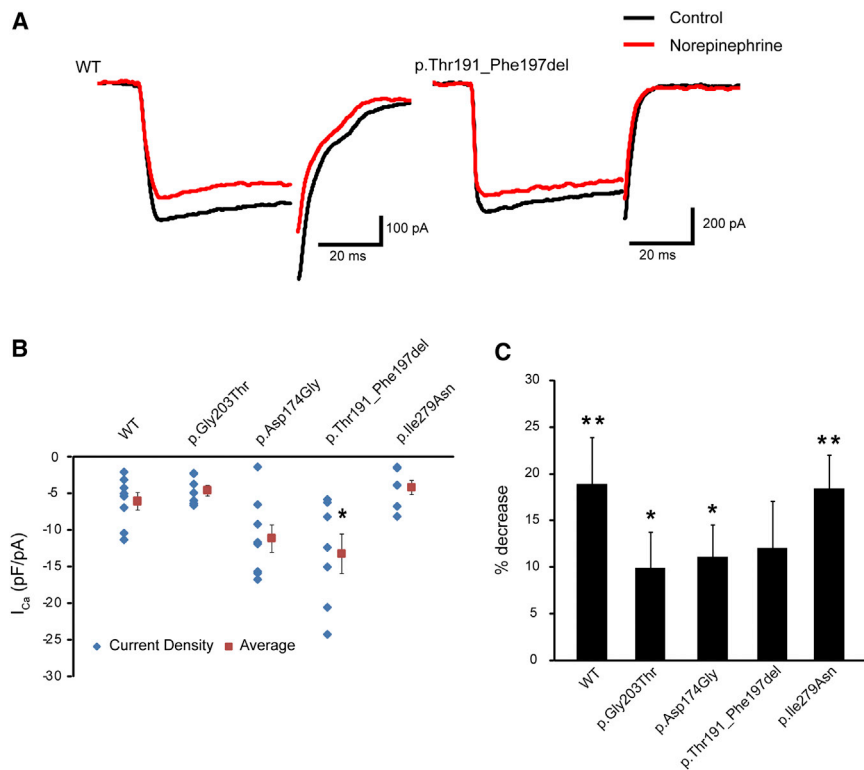


Figure 5. Evaluation of $G\alpha_o$ -Mediated Signaling in NG108-15 Cell Calcium-Current Generation

(A) Representative traces of voltage-gated calcium currents generated in NG108-15 cells expressing WT (left) or p.Thr191_Phe197del altered (right) $G\alpha_{o1}$. Black and red traces represent the currents before and 3 min after application of 10 μ M norepinephrine, respectively.

(B) Current densities of the calcium currents before norepinephrine treatment in cells expressing WT or altered $G\alpha_{o1}$. Scatter plots represent the densities in individual cells. Red squares and bars represent the means and SEMs, respectively, of the densities in individual cell groups (WT, $n = 8$; p.Gly203Thr, $n = 7$; p.Asp174Gly, $n = 8$; p.Thr191_Phe197del, $n = 7$; p.Ile279Asn, $n = 7$). Compared with that in cells expressing WT $G\alpha_{o1}$, the current density in cells expressing p.Thr191_Phe197del increased significantly (* $p < 0.05$ by Dunnett's post hoc test). The densities in the cells expressing other altered proteins did not vary significantly.

(C) Comparison of norepinephrine-induced inhibition of calcium currents in cells expressing altered $G\alpha_{o1}$. Each error bar represents the mean and SEM of the percent decrease in current density

induced by application of 10 μ M norepinephrine. Paired t tests indicated that the inhibition induced by norepinephrine was significant in cells expressing WT ($n = 8$) and p.Gly203Thr ($n = 7$), p.Asp174Gly ($n = 8$), and p.Ile279Asn ($n = 7$) altered proteins (** $p < 0.01$ and * $p < 0.05$), but not in cells expressing p.Thr191_Phe197del ($n = 7$). Although there was some tendency for decreased inhibition in cells expressing altered proteins, the tendency did not reach statistical significance compared with that in WT-expressing cells ($p = 0.41$ by ANOVA).

and p.Asp174Gly) also showed weak signal in the cytosol, suggesting that localization to the plasma membrane was variably impaired in three altered proteins. Measurement of voltage-dependent calcium currents in NG108-15 cells also suggested impaired functions of altered $G\alpha_{o1}$. The p.Thr191_Phe197del alteration significantly increased the basal calcium-current density, and compared with WT-expressing cells, cells expressing one of the three substitutions (p.Thr191_Phe197del, p.Asp174Gly, or p.Gly203Thr) showed a tendency towards weaker inhibition of calcium currents by norepinephrine. All these data suggest that the four *GNAO1* mutations might cause loss of $G\alpha_{o1}$ function.

Our experimental data suggest that $G\alpha_o$ function might be most severely affected in the p.Thr191_Phe197del altered protein. This appears to be correlated with the severity of clinical features because individual 3 showed both OS and involuntary movements and indeed died during the infantile period. Therefore, she might have had the most severe phenotype caused by a *GNAO1* mutation. Another interesting finding is somatic mosaicism of the c.521A>G (p.Asp174Gly) mutation in individual 2, in whom approximately 35%–50% of cells harbored the mutation. Somatic mosaicism of responsive genes in infantile epilepsy, such as *SCN1A* (MIM 182389) and *STXBP1*, have been reported, explaining the presence of unaffected

or mildly affected transmitting parents.^{30,31} However, individual 2 showed OS, delayed myelination, and thin corpus callosum. Although we did not determine the mosaic rate in brain tissues, the presence of 35%–50% of cells harboring the *GNAO1* mutation in the brain might be sufficient to cause abnormal brain development.

It has been reported that activation of G-protein-coupled α_2 adrenergic receptors by norepinephrine attenuates epileptiform activity in the hippocampal CA3 region.³² $G\alpha_o$ is known to be involved in this response,³³ suggesting that alteration of pathways mediated by α_2 adrenergic receptor and $G\alpha_o$ might contribute to the pathogenesis of epilepsy. Because calcium-current inhibition is a well-known consequence of $G\alpha_o$ -mediated signaling induced by norepinephrine, it is possible that epileptic seizures associated with *GNAO1* mutations might be improved by calcium-channel modulators. For example, pregabalin and gabapentin act as selective calcium-channel blockers,^{34,35} and topiramate modulates high-voltage-activated calcium channels in dentate granule cells.³⁶ Because our four individuals were not treated with these drugs, it is worth administrating these three drugs for examining putative protective effects.

In conclusion, de novo heterozygous *GNAO1* mutations were identified in four individuals with epileptic encephalopathy. Furthering our understanding of abnormal

G α_o -mediated heterotrimeric G protein signaling might provide new insights into the pathogenesis and treatment of epileptic encephalopathy.

Supplemental Data

Supplemental Data include two figures, three tables, and one movie and can be found with this article online at <http://www.cell.com/AJHG>.

Acknowledgments

We would like to thank the individuals and their families for their participation in this study. We also thank Aya Narita and Nobuko Watanabe for their technical assistance and Tohru Kozasa and Nobuchika Suzuki for their valuable comments. This work was supported by the Ministry of Health, Labour, and Welfare of Japan, the Japan Society for the Promotion of Science (Grants-in-Aid for Scientific Research (B) [25293085 and 25293235] and a Grant-in-Aid for Scientific Research (A) [13313587]), the Takeda Science Foundation, the Japan Science and Technology Agency, the Strategic Research Program for Brain Sciences (11105137), and a Grant-in-Aid for Scientific Research on Innovative Areas (Transcription Cycle) from the Ministry of Education, Culture, Sports, Science, and Technology of Japan (12024421).

Received: May 17, 2013

Revised: July 9, 2013

Accepted: July 17, 2013

Published: August 29, 2013

Web Resources

The URLs for data presented herein are as follows:

CLUSTALW, <http://www.genome.jp/tools/clustalw/>

GenBank, <http://www.ncbi.nlm.nih.gov/Genbank/>

NHLBI Exome Sequencing Project (ESP) Exome Variant Server, <http://evs.gs.washington.edu/EVS/>

Online Mendelian Inheritance in Man (OMIM), <http://www.omim.org/>

Picard, <http://picard.sourceforge.net/>

Protein Data Bank, <http://www.rcsb.org/pdb/home/home.do>

PyMOL, www.pymol.org

RefSeq, <http://www.ncbi.nlm.nih.gov/RefSeq>

UniProtKB/Swiss-Prot, <http://www.uniprot.org/>

References

1. Dulac, O. (2001). Epileptic encephalopathy. *Epilepsia* 42 (Suppl 3), 23–26.
2. Ohtahara, S., and Yamatogi, Y. (2006). Ohtahara syndrome: with special reference to its developmental aspects for differentiating from early myoclonic encephalopathy. *Epilepsy Res.* 70 (Suppl 1), S58–S67.
3. Saitsu, H., Kato, M., Koide, A., Goto, T., Fujita, T., Nishiyama, K., Tsurusaki, Y., Doi, H., Miyake, N., Hayasaka, K., and Matsumoto, N. (2012). Whole exome sequencing identifies KCNQ2 mutations in Ohtahara syndrome. *Ann. Neurol.* 72, 298–300.
4. Saitsu, H., Kato, M., Mizuguchi, T., Hamada, K., Osaka, H., Tohyama, J., Uruno, K., Kumada, S., Nishiyama, K., Nishimura, A., et al. (2008). *De novo* mutations in the gene encoding STXBP1 (MUNC18-1) cause early infantile epileptic encephalopathy. *Nat. Genet.* 40, 782–788.
5. Weckhuysen, S., Mandelstam, S., Suls, A., Audenaert, D., Deconinck, T., Claes, L.R., Deprez, L., Smets, K., Hristova, D., Yordanova, I., et al. (2012). KCNQ2 encephalopathy: emerging phenotype of a neonatal epileptic encephalopathy. *Ann. Neurol.* 71, 15–25.
6. Kato, M., Saitoh, S., Kamei, A., Shiraishi, H., Ueda, Y., Akasaka, M., Tohyama, J., Akasaka, N., and Hayasaka, K. (2007). A longer polyalanine expansion mutation in the ARX gene causes early infantile epileptic encephalopathy with suppression-burst pattern (Ohtahara syndrome). *Am. J. Hum. Genet.* 81, 361–366.
7. Wettschureck, N., and Offermanns, S. (2005). Mammalian G proteins and their cell type specific functions. *Physiol. Rev.* 85, 1159–1204.
8. Huff, R.M., Axton, J.M., and Neer, E.J. (1985). Physical and immunological characterization of a guanine nucleotide-binding protein purified from bovine cerebral cortex. *J. Biol. Chem.* 260, 10864–10871.
9. Valenzuela, D., Han, X., Mende, U., Fankhauser, C., Mashimo, H., Huang, P., Pfeiffer, J., Neer, E.J., and Fishman, M.C. (1997). G α_o is necessary for muscarinic regulation of Ca $^{2+}$ channels in mouse heart. *Proc. Natl. Acad. Sci. USA* 94, 1727–1732.
10. Jiang, M., Gold, M.S., Boulay, G., Spicher, K., Peyton, M., Brabet, P., Srinivasan, Y., Rudolph, U., Ellison, G., and Birnbaumer, L. (1998). Multiple neurological abnormalities in mice deficient in the G protein Go. *Proc. Natl. Acad. Sci. USA* 95, 3269–3274.
11. Saitsu, H., Kato, M., Osaka, H., Moriyama, N., Horita, H., Nishiyama, K., Yoneda, Y., Kondo, Y., Tsurusaki, Y., Doi, H., et al. (2012). CASK aberrations in male patients with Ohtahara syndrome and cerebellar hypoplasia. *Epilepsia* 53, 1441–1449.
12. Saitsu, H., Nishimura, T., Muramatsu, K., Koderia, H., Kumada, S., Sugai, K., Kasai-Yoshida, E., Sawaura, N., Nishida, H., Hoshino, A., et al. (2013). *De novo* mutations in the autophagy gene WDR45 cause static encephalopathy of childhood with neurodegeneration in adulthood. *Nat. Genet.* 45, 445–449, e1.
13. DePristo, M.A., Banks, E., Poplin, R., Garimella, K.V., Maguire, J.R., Hartl, C., Philippakis, A.A., del Angel, G., Rivas, M.A., Hanna, M., et al. (2011). A framework for variation discovery and genotyping using next-generation DNA sequencing data. *Nat. Genet.* 43, 491–498.
14. Wang, K., Li, M., and Hakonarson, H. (2010). ANNOVAR: functional annotation of genetic variants from high-throughput sequencing data. *Nucleic Acids Res.* 38, e164.
15. Robinson, J.T., Thorvaldsdóttir, H., Winckler, W., Guttman, M., Lander, E.S., Getz, G., and Mesirov, J.P. (2011). Integrative genomics viewer. *Nat. Biotechnol.* 29, 24–26.
16. Thorvaldsdóttir, H., Robinson, J.T., and Mesirov, J.P. (2013). Integrative Genomics Viewer (IGV): high-performance genomics data visualization and exploration. *Brief. Bioinform.* 14, 178–192.
17. Slepak, V.Z., Wilkie, T.M., and Simon, M.I. (1993). Mutational analysis of G protein alpha subunit G(o) alpha expressed in *Escherichia coli*. *J. Biol. Chem.* 268, 1414–1423.
18. Williams, D.J., Puhl, H.L., and Ikeda, S.R. (2010). A Simple, Highly Efficient Method for Heterologous Expression in Mammalian Primary Neurons Using Cationic Lipid-mediated mRNA Transfection. *Front Neurosci.* 4, 181.

19. Guerois, R., Nielsen, J.E., and Serrano, L. (2002). Predicting changes in the stability of proteins and protein complexes: a study of more than 1000 mutations. *J. Mol. Biol.* **320**, 369–387.
20. Wall, M.A., Coleman, D.E., Lee, E., Iñiguez-Lluhi, J.A., Posner, B.A., Gilman, A.G., and Sprang, S.R. (1995). The structure of the G protein heterotrimer Gi alpha 1 beta 1 gamma 2. *Cell* **83**, 1047–1058.
21. Rasmussen, S.G., DeVree, B.T., Zou, Y., Kruse, A.C., Chung, K.Y., Kobilka, T.S., Thian, F.S., Chae, P.S., Pardon, E., Calinski, D., et al. (2011). Crystal structure of the β_2 adrenergic receptor-Gs protein complex. *Nature* **477**, 549–555.
22. Waldo, G.L., Ricks, T.K., Hicks, S.N., Cheever, M.L., Kawano, T., Tsuboi, K., Wang, X., Montell, C., Kozasa, T., Sondek, J., and Harden, T.K. (2010). Kinetic scaffolding mediated by a phospholipase C-beta and Gq signaling complex. *Science* **330**, 974–980.
23. Edvardson, S., Baumann, A.M., Mühlenhoff, M., Stephan, O., Kuss, A.W., Shaag, A., He, L., Zenvirt, S., Tanzi, R., Gerardy-Schahn, R., and Elpeleg, O. (2013). West syndrome caused by ST3Gal-III deficiency. *Epilepsia* **54**, e24–e27.
24. Molinari, F., Raas-Rothschild, A., Rio, M., Fiermonte, G., Encha-Razavi, F., Palmieri, L., Palmieri, F., Ben-Neriah, Z., Kadhom, N., Vekemans, M., et al. (2005). Impaired mitochondrial glutamate transport in autosomal recessive neonatal myoclonic epilepsy. *Am. J. Hum. Genet.* **76**, 334–339.
25. Mills, P.B., Surtees, R.A., Champion, M.P., Beesley, C.E., Dalton, N., Scambler, P.J., Heales, S.J., Briddon, A., Scheimberg, I., Hoffmann, G.F., et al. (2005). Neonatal epileptic encephalopathy caused by mutations in the PNPO gene encoding pyridox(am)ine 5'-phosphate oxidase. *Hum. Mol. Genet.* **14**, 1077–1086.
26. Shen, J., Gilmore, E.C., Marshall, C.A., Haddadin, M., Reynolds, J.J., Eyaid, W., Bodell, A., Barry, B., Gleason, D., Allen, K., et al. (2010). Mutations in PNKP cause microcephaly, seizures and defects in DNA repair. *Nat. Genet.* **42**, 245–249.
27. Kurian, M.A., Meyer, E., Vassallo, G., Morgan, N.V., Prakash, N., Pasha, S., Hai, N.A., Shuib, S., Rahman, F., Wassmer, E., et al. (2010). Phospholipase C beta 1 deficiency is associated with early-onset epileptic encephalopathy. *Brain* **133**, 2964–2970.
28. Nakata, H., and Kozasa, T. (2005). Functional characterization of Galphao signaling through G protein-regulated inducer of neurite outgrowth 1. *Mol. Pharmacol.* **67**, 695–702.
29. McFadzean, I., Mullaney, I., Brown, D.A., and Milligan, G. (1989). Antibodies to the GTP binding protein, Go, antagonize noradrenaline-induced calcium current inhibition in NG108-15 hybrid cells. *Neuron* **3**, 177–182.
30. Saitsu, H., Hoshino, H., Kato, M., Nishiyama, K., Okada, I., Yoneda, Y., Tsurusaki, Y., Doi, H., Miyake, N., Kubota, M., et al. (2011). Paternal mosaicism of an *STXBPI* mutation in OS. *Clin. Genet.* **80**, 484–488.
31. Marini, C., Scheffer, I.E., Nabbout, R., Suls, A., De Jonghe, P., Zara, F., and Guerrini, R. (2011). The genetics of Dravet syndrome. *Epilepsia* **52** (Suppl 2), 24–29.
32. Jurgens, C.W., Hammad, H.M., Lichter, J.A., Boese, S.J., Nelson, B.W., Goldenstein, B.L., Davis, K.L., Xu, K., Hillman, K.L., Porter, J.E., and Doze, V.A. (2007). Alpha2A adrenergic receptor activation inhibits epileptiform activity in the rat hippocampal CA3 region. *Mol. Pharmacol.* **71**, 1572–1581.
33. Goldenstein, B.L., Nelson, B.W., Xu, K., Luger, E.J., Pribula, J.A., Wald, J.M., O'Shea, L.A., Weinshenker, D., Charbeneau, R.A., Huang, X., et al. (2009). Regulator of G protein signaling protein suppression of Galphao protein-mediated alpha2A adrenergic receptor inhibition of mouse hippocampal CA3 epileptiform activity. *Mol. Pharmacol.* **75**, 1222–1230.
34. Sills, G.J. (2006). The mechanisms of action of gabapentin and pregabalin. *Curr. Opin. Pharmacol.* **6**, 108–113.
35. Stefani, A., Spadoni, F., Giacomini, P., Lavaroni, F., and Bernardi, G. (2001). The effects of gabapentin on different ligand- and voltage-gated currents in isolated cortical neurons. *Epilepsy Res.* **43**, 239–248.
36. Zhang, X., Velumian, A.A., Jones, O.T., and Carlen, P.L. (2000). Modulation of high-voltage-activated calcium channels in dentate granule cells by topiramate. *Epilepsia* **41** (Suppl 1), S52–S60.